Investigation into the synergistic effect of atorvastatin combined with ultrasound stimulation for anti-glioma therapy

MENG TING LIN[1,2], TSAI-YUN CHAN[2], WEI-HAO LIAO[2], CHUEH-HUNG WU[2,3], TAI-HORNG YOUNG[1] and WEN-SHIANG CHEN[2]

[1]Department of Biomedical Engineering, College of Medicine, National Taiwan University, Taipei 100, Taiwan, R.O.C.; [2]Department of Physical Medicine and Rehabilitation, National Taiwan University Hospital, College of Medicine, National Taiwan University, Taipei 100, Taiwan, R.O.C.; [3]Department of Physical Medicine and Rehabilitation, National Taiwan University Hospital Hsin-Chu Branch, Hsinchu 300, Taiwan, R.O.C.

Received February 24, 2025; Accepted July 10, 2025

DOI: 10.3892/ol.2025.15213

Abstract. Glioblastoma (GBM) is an aggressive, malignant brain tumor marked by rapid growth and invasiveness. Ultrasound (US) stimulation has emerged as a potential therapeutic approach for the management of GBM. Atorvastatin (ATO), a drug widely used to treat hyperlipidemia, has also been recognized for its anticancer properties, including inhibition of cell proliferation, induction of cell cycle arrest and promotion of apoptosis. Despite these promising attributes, the combined effectiveness of ATO and US stimulation in GBM treatment remains unclear. The present study aimed to explore the potential synergistic effects of ATO and US stimulation on C6 glioma cells. The optimal concentration of ATO and calibrated US parameters were determined in the present study. The cells were treated with ATO or US, followed by assessments of cellular viability and reactive oxygen species (ROS) to establish the most effective ATO dose and US parameters. The cells were then treated with ATO, US or their combination, and cellular viability, ROS levels, ATP production, tumor cell migration and the impact on downstream molecular pathways, particularly the AKT/mTOR signaling pathway, which is key for cell survival and proliferation, were assessed. The present findings revealed that ATO independently suppressed glioma cell viability by elevating ROS levels and reducing ATP production, and it showed a trend toward impairing tumor cell migration. These effects were notably associated with downregulation of the AKT axis, which indicated disruption of key survival mechanisms within the tumor cells. However, the anticipated synergistic effect of combining ATO with US stimulation was not observed under the tested conditions, thus suggesting that US stimulation did not further augment the therapeutic effect of ATO. While the combination therapy did not yield additive benefits, ATO alone exhibited notable potential as a therapeutic agent against glioma. In conclusion, the present study highlighted the need for further research on the role of ATO to further harness its anticancer properties in the context of GBM treatment.

Correspondence to: Professor Tai-Horng Young, Department of Biomedical Engineering, College of Medicine, National Taiwan University, 1, Section 1, Jen-Ai Road, Taipei 100, Taiwan, R.O.C.
E-mail: thyoung@ntu.edu.tw

Professor Wen-Shiang Chen, Department of Physical Medicine and Rehabilitation, National Taiwan University Hospital, College of Medicine, National Taiwan University, 1, Section 1, Ren'ai Road, Zhongzheng, Taipei 100, Taiwan, R.O.C.
E-mail: wenshiang@gmail.com

Key words: glioma, atorvastatin, ultrasound

Introduction

Glioma is a common brain tumor arising from astrocytes, with glioblastoma [GBM; ICD-10 code C71.9 (1) representing its most malignant form. GBM accounts for 15% of all brain tumors (2) and is characterized by rapid growth and high recurrence, with a median progression-free survival of 15 months and a high mortality rate (5-year survival rate, 5.5%) (2). Its highly invasive nature often causes elevated intracranial pressure and compression of surrounding brain structures, which results in progressive neurological symptoms such as hemiplegia, aphasia, blurred vision and seizures (3). Despite standard treatment involving surgical resection followed by chemotherapy and/or radiotherapy, the recurrence rate remains high and the average survival time for patients is <1 year (4). One of the major challenges in GBM chemotherapy is the presence of the blood-brain barrier (BBB), which restricts drug delivery to the tumor site. This limitation reduces the drug concentration in the target area, which potentially contributes to drug resistance and ultimately leads to treatment failure (5).

Ultrasonic stimulation has been developed as a treatment modality for brain tumors in preclinical studies (6-9). In addition to the thermal effect, ultrasound (US) can generate non-thermal effects, such as cavitation, microstreaming and sonoporation, particularly when combined with US contrast agents (UCAs), which facilitate the temporary opening of the BBB (10,11). *In vitro* studies have demonstrated that sonoporation induced by US not only enhances cellular permeability to facilitate drug delivery but also generates free radicals and

reactive oxygen species (ROS) (12,13), which lead to mitochondrial damage and apoptosis (14). In addition, increased ROS production following US exposure has been shown to effectively induce C6 glioma cell death (6,7). Furthermore, the combination of US and UCAs has been reported to increase the concentration of temozolomide in the brain via BBB opening and reduce glioma progression in animal studies (8,9).

Atorvastatin (ATO), a 3-hydroxy-3-methyl-glutaryl (HMG)-CoA reductase inhibitor, is widely used for its antihyperlipidemic effect and in the secondary prevention of cardiovascular diseases, including ischemic stroke and myocardial infarction (15). In animal experiments, statins including ATO have been shown to exert an anti-glioma effect by inhibiting glioma cell proliferation, migration and cell cycle progression, as well as by inducing apoptosis (16). Statins exert these effects by blocking the mevalonate pathway and thus modulating downstream signaling pathways, such as Ras/Raf/ERK, PI3K/AKT and NF-κB, which are involved in autophagy and metastasis (16). Moreover, ATO has been reported to augment the anticancer effect of temozolomide through Ras and ERK-related mechanisms to inhibit tumor growth (17). Clinical studies have further revealed that statins may improve long-term survival in patients with GBM and reduce the incidence of brain tumors (18,19). Furthermore, while ATO has been reported to reduce ROS levels in cardiac muscle, it has also been associated with increased oxidative stress in skeletal muscle cells and oral squamous cell carcinoma (20-22).

The AKT/PI3K/mTOR signaling pathway and the generation of ROS serve key roles in the pathophysiology and therapeutic resistance of GBM. Hyperactivation of the PI3K/AKT/mTOR pathway is one of the most frequently observed molecular abnormalities in GBM, largely due to mutations or loss of the tumor suppressor PTEN, which negatively regulates this signaling cascade (23). Targeting the redox balance in GBM cells, for example, by inhibition of antioxidant systems such as the glutathione or thioredoxin pathways, or by increasing ROS production, can sensitize tumors to therapy (24). An *in vitro* study demonstrated that inducing ROS generation in GBM cells subsequently suppresses AKT/mTOR pathway activity, which can lead to the induction of both apoptosis and autophagy. Notably, inhibition of ROS has been shown to attenuate these effects, thus confirming that ROS operates upstream in this regulatory axis (25). Similarly, Zhang *et al* (26) revealed that inhibition of cathepsin S elevated intracellular ROS, concurrently inhibiting PI3K/AKT/mTOR signaling, resulting in autophagy and mitochondrial apoptosis in GBM cells, whereas the blockade of autophagy suppressed apoptosis, thus indicating that autophagy facilitates GBM cell death under oxidative stress. Complementing these findings, Yin *et al* (27) investigated the sensitization of GBM cells to temozolomide by curcumin and reported that the combination treatment markedly elevated ROS levels and enhanced inhibition of the AKT/mTOR axis compared with monotherapy; this synergistic enhancement of ROS production and signaling disruption led to increased apoptosis both *in vitro* and *in vivo*. Taken together, these mechanisms highlight the rationale for the investigation of agents such as ATO and US, which have been reported to modulate both ROS levels and the AKT/mTOR pathway, as potential adjuvants in GBM treatment strategies.

However, it remains unclear whether ROS generation and cellular death induced by US and ATO can produce a synergistic anti-glioma effect. Therefore, the present study aimed to investigate the therapeutic potential of combining ATO with US stimulation and to elucidate the downstream mechanism involved in glioma cell suppression.

Materials and methods

Cell culture. As an *in vitro* model, rat C6 glioma cells (Bioresource Collection and Research Center) were cultured in high-glucose DMEM (containing 4.5 g/l glucose; Gibco; Thermo Fisher Scientific, Inc.) supplemented with 10% FBS (Invitrogen; Thermo Fisher Scientific, Inc.). The cells were grown in a monolayer at 37˚C in a 5% CO_2 humidified incubator. All experiments were conducted using cells at passages 3-6 to ensure reproducibility and to minimize variability in cellular behavior. Cells were trypsinized after reaching 70-80% confluence and were seeded in 24- and 96-well plates according to the subsequent experiments.

ATO preparation. ATO calcium ($C_{66}H_{68}CaF_2N_4O_{10}\cdot 3H_2O$) was purchased from MilliporeSigma (cat. no. PHR1422). ATO was diluted in DMSO to obtain different concentrations (1-10 μM) and to determine the optimal cancericidal effect. The concentrations were selected based on prior studies in glioma cells (28,29). A pilot study was conducted to determine the optimal concentration of ATO based on cell viability and morphology, aiming for ~70% viability without noticeable cellular death. In the initial pilot experiment, cell survival was assessed across a range of 0-10 μM ATO and a marked reduction in viability was observed at concentrations >5 μM, accompanied by marked morphological signs of cell death observed under a light microscope (Fig. 1B and C). Consequently, the ATO concentration range was refined to 1-5 μM and it was revealed that 2-3 μM ATO provided the optimal balance, maintaining cell viability without inducing evident morphological damage (Fig. 1D and E), and this range was thus selected for subsequent experiments. DMSO concentration was kept at <0.1% in all groups and controlled accordingly. The best concentration of ATO, determined to be 3 μM, was utilized for subsequent experiments.

US stimulation. A US device with a planar piezoelectric transducer (ITO US-700; ITO Physiotherapy & Rehabilitation) was used for stimulation. The parameters of US were set as 1 MHz, 0-3 W/cm^2, 5-20% duty cycle and 2 min stimulation. Best ultrasound intensity (high-intensity US: 1 MHz, 1.5 W/cm^2, duty cycle 5%, 2 min stimulation at room temperature; or low-intensity US: 1 MHz, 0.2 W/cm^2, duty cycle 20%, 2 min stimulation at room temperature) were adopted in subsequent experiments. The US stimulation settings were similar to those in our previous study (frequency of 1 MHz and intensity of 0-0.8 W/cm^2) to facilitate non-thermal bioeffects, such as cavitation (14,30). Regarding the choice of frequency and intensity, Hao *et al* (6) demonstrated that US at a frequency of 0.5-1 MHz and intensity of 1 W/cm^2 induced apoptosis in C6 glioma cells through ROS generation and calcium overload. Similarly, Li *et al* (7) applied US at 1 MHz and 0.5 W/cm^2 and observed notable ROS production and inhibition of C6

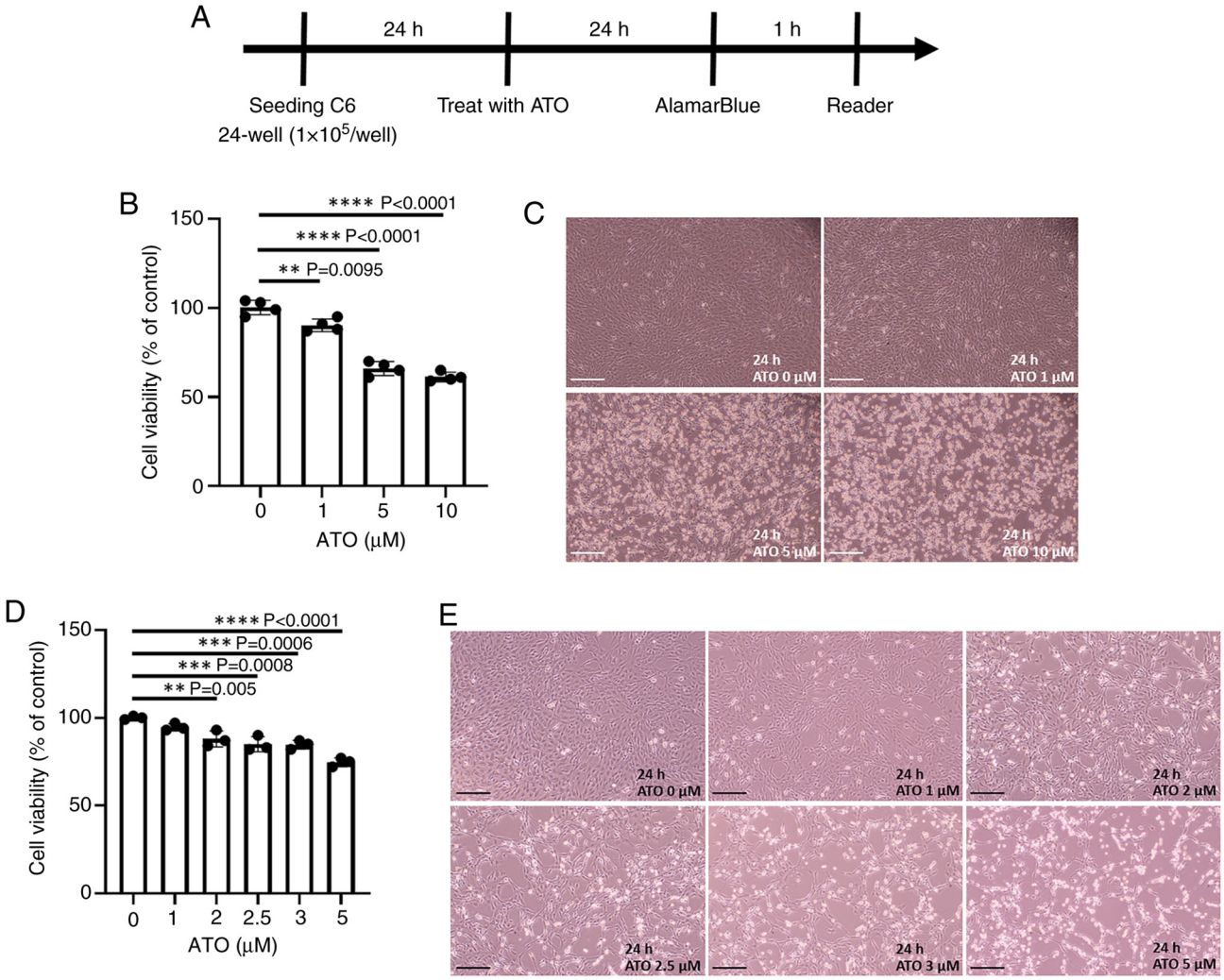

Figure 1. Effect of ATO on the viability of C6 glioma cells. (A) Flow diagram. Effects of 1, 5 and 10 μM ATO on cell (B) viability (n=4) and (C) morphology at 24 h. (D) Extended dose-response analysis at 24 h, which demonstrated survival rates (n=3) and (E) cellular morphology following treatment with 1, 2, 2.5, 3 and 5 μM ATO. Scale bar, 200 μm. **P<0.01, ***P<0.001, ****P<0.0001. ATO, atorvastatin.

cell proliferation. Based on these previous studies, the present study selected a frequency of 1 MHz and an intensity range of 0-3 W/cm^2 to optimize ROS generation. A fixed central frequency of 1 MHz ensured consistent acoustic conditions across all treatment groups (14,30), which allowed for controlled comparison of different intensity effects while minimizing variability associated with frequency modulation. Briefly, the well of the plate was placed in a tank filled with degassed water and sonicated at the center of the transducer; in order to deliver uniform mechanical wave, the bottom of the plate was placed perpendicularly to the probe with a 12.0-cm distance after calculating the near field length of the transducer (30). Sonazoid™ (Cytiva) was applied in conjunction with US to induce non-thermal bioeffects including acoustic cavitation and tumor cell microstreaming. Prior to US exposure, the concentration and spatial distribution of Sonazoid microbubbles were evaluated using bright-field microscopy. Images of multiple representative fields per well were captured and microbubble density was quantified using MATLAB software (version 9.9, R2020b; The MathWorks, Inc.) to ensure a consistent concentration of 1x10^8 microbubbles/mm^2 across experimental wells. A total of 5 μl Sonazoid was added to each well containing 0.5 ml culture medium, based on standard protocols for microbubble preparation. A control group was prepared with Sonazoid alone, without subsequent US stimulation, to evaluate its baseline effect independent of acoustic exposure. The subsequent tests were performed after US stimulation. An infrared thermometer (TM-909AL; Lutron Electronics Co., Inc.) was used to measure the temperature.

Cell viability assay. C6 cell survival after anti-glioma treatment was measured with the AlamarBlue™ cell viability assay (Thermo Fisher Scientific Inc.). Cells were placed in 24-well plates with 1 ml culture medium (7.5x10^4-1x10^5 cells/well). Cells (1x10^5 cells/well) were treated with ATO (0-10 μM for 24 h at 37˚C) to determine the optimal cancericidal effect, and cells (7.5x10^4 cells/well) were also treated with ATO (0-10 μM for 24 h at 37˚C) with high- or low-intensity US. Subsequently, the cells were incubated for 24 h and then washed twice with PBS. AlamarBlue working solution was prepared by diluting the reagent 1:10 (v/v) in fresh culture medium. A total of 1 ml of this solution was added to each well and incubated at 37˚C and 5% CO_2 for 1 h. To account for background fluorescence and control inter-well variability, blank wells

containing only AlamarBlue working solution and medium (without cells) were included in each assay plate. Fluorescence intensity (excitation/emission 530/590 nm) was recorded using a microplate spectrophotometer (Infinite M200; Tecan Group, Ltd.). Background-subtracted fluorescence values were used to calculate relative cell viability (%) as follows: $(RFU_{treatment}-RFU_{blank})/(RFU_{control}-RFU_{blank})$ x100. Each test was performed at least in triplicate and a minimum of three tests was conducted on separate days.

ROS quantification. To detect the intracellular accumulation of hydrogen peroxide (H_2O_2), and thus ROS levels, a 10 mM 2',7'-dichlorodihydrofluorescein diacetate (DCFDA) stock solution (MilliporeSigma) was prepared. Briefly, C6 cells ($1.5x10^5$/well; 1 ml) were incubated with 10 μM DCFDA for 30 min at 37˚C and subsequently underwent US according to the aforementioned settings (1 MHz, 0-3 W/cm^2) to determine the best US parameter. Next, the cells were treated with 0-3 μM ATO for 24 h at 37˚C, followed by treatment with or without high-intensity US in 24-well plates. The cells were then immediately trypsinized and analyzed by flow cytometry (LSRII; BD Biosciences) and FlowJo software (v7.6; Becton, Dickinson & Company). Each experiment was performed at least in triplicate and a minimum of three experiments was conducted.

ATP detection. ATP serves a key role in cellular metabolism and can be used to determine mitochondrial function, as well as extent of cellular damage or death (31,32). Cellular ATP levels were measured using the Luminescent ATP Detection Assay Kit (cat. no. ab113849; Abcam) as per the manufacturer's protocol. Briefly, 1 ml (10^5 cells/ml) cells in a 24-well plate received treatments: high-intensity US, ATO (3 μM for 24 h at 37˚C), ATO + US or control (0.1% DMSO), and were then immediately lysed in 50 μl detergent from the Luminescent ATP Detection Assay Kit. Subsequently, substrate buffer (50 μl) was added and luminescence was detected using a microplate spectrophotometer (Infinite M200; Tecan Group, Ltd.). H_2O_2 was used as a positive control. At least three experiments were performed and each experiment was conducted at least in triplicate.

Tumor cell migration. The migration of C6 cells was assessed using a gap closure assay. Briefly, 70 μl cells ($3x10^5$/ml) were seeded in each well of an Ibidi Culture-Insert (Ibidi GmbH) inside a 24-well plate and were cultured in DMEM supplemented with 1% FBS [this concentration of FBS was used to avoid cell proliferation (33)] for 24 h at 37˚C under 5% CO_2. Before US stimulation, 1 μl Sonazoid was added to each well of the Ibidi Culture-Insert. After being exposed for 4 h, the Ibidi Culture-Insert was removed to leave a constant cell-free gap. Cells were treated with ATO (concentrations 0, 1, 2 and 3 μM for 18 h at 37˚C) with or without US (1 MHz, 1 W/cm^2, duty cycle 20%, 2 min stimulation at room temperature), and were then incubated for 18 h under the aforementioned conditions. Cell migration coverage was visualized using an inverted light microscope (IX71; Olympus Corporation) and was analyzed using ImageJ software (v1.54g; National Institutes of Health). Tumor migration was calculated using the formula: Migration coverage $_{\text{initial area}}$-Migration coverage $_{\text{area at 18 h}}$/Migration coverage $_{\text{initial area}}$ (34).

Western blot analysis. The cells ($1x10^5$/ml) were treated with different regimens: High-intensity US, ATO (3 μM for 24 h at 37˚C), ATO + US or control. After exposure, the cells were placed in an incubator for 10 min at 37˚C. RIPA lysis buffer (cat. no. 89900; Thermo Fisher Scientific, Inc.) was used for cell lysis and the samples were subsequently centrifuged at 13,000 x g for 10 min at 4˚C. The protein concentration was determined using the Bradford protein assay. After denaturation, the proteins (20 μg) were separated by electrophoresis on 4-12% precast polyacrylamide gels (cat. no. NW04125BOX; Invitrogen; Thermo Fisher Scientific, Inc.), and were transferred to PVDF membranes (MilliporeSigma). After transfer, the membranes were blocked in BlockPRO™ 1 Min Protein-Free Blocking Buffer (cat. no. BM01; Visual Protein; ENERGENESIS BIOMEDICAL CO., LTD.) for 1 min at room temperature. The membranes were incubated with the following primary antibodies diluted in SignalBoost™ Immunoreaction Enhancer Kit (cat. no. 407207; MilliporeSigma) overnight at 4˚C: Rabbit anti-phosphorylated (p)-mTOR (Ser2448) antibody (1:2,000 dilution; cat. no. GTX132803; GeneTex, Inc.), rabbit anti-mTOR antibody (1:3,000 dilution; cat. no. GTX101557; GeneTex, Inc.), rabbit anti-p-AKT (Ser473) antibody (1:2,000 dilution; cat. no. GTX128414; GeneTex, Inc.) and rabbit anti-AKT antibody (1:3,000 dilution; cat. no. GTX121937; GeneTex, Inc.), then with a HRP-conjugated goat anti-rabbit IgG heavy and light chain cross-adsorbed secondary antibody (1:5,000 dilution; cat. no. A120-201P; Fortis Life Sciences) for 1 h at room temperature. To confirm equal protein loading and normalization, the membranes were probed with an anti-GAPDH antibody (1:10,000 dilution; cat. no. 60004-1-Ig; Proteintech Group, Inc.) as a loading control, after which, the membranes were probed with a HRP-conjugated goat anti-mouse IgG heavy and light chain cross-adsorbed secondary antibody (1:10,000 dilution; cat. no. A90-216P; Fortis Life Sciences, LLC) for 1 h at room temperature. Finally, western blotting was visualized using Amersham™ ECL select western blotting detection reagent (Cytiva), images were recorded using the UVP BioSpectrum Image system (Analytik Jena AG) and were analyzed by ImageJ software (v1.54g; National Institutes of Health) as in a previous study (35).

Statistical analysis. All continuous data are presented as the mean ± standard deviation. One-way ANOVA with Tukey's post hoc test was used for comparisons among multiple groups. $P<0.05$ was considered to indicate a statistically significant difference. Statistical analysis was performed using SPSS (version 15.0; SPSS, Inc.).

Results

Effect of ATO on the viability and ROS levels of C6 glioma cells. A flow diagram of the experimental protocol is shown in Fig. 1A. After 24 h of treatment with ATO, the viability of C6 cells was assessed using the AlamarBlue assay. As shown in Fig. 1B, cell survival in the 1, 5 and 10 μM ATO-treated groups was significantly lower compared with that in the untreated group, with the reduction becoming more pronounced as the ATO concentration increased ($P=0.0095$ for 1 μM and

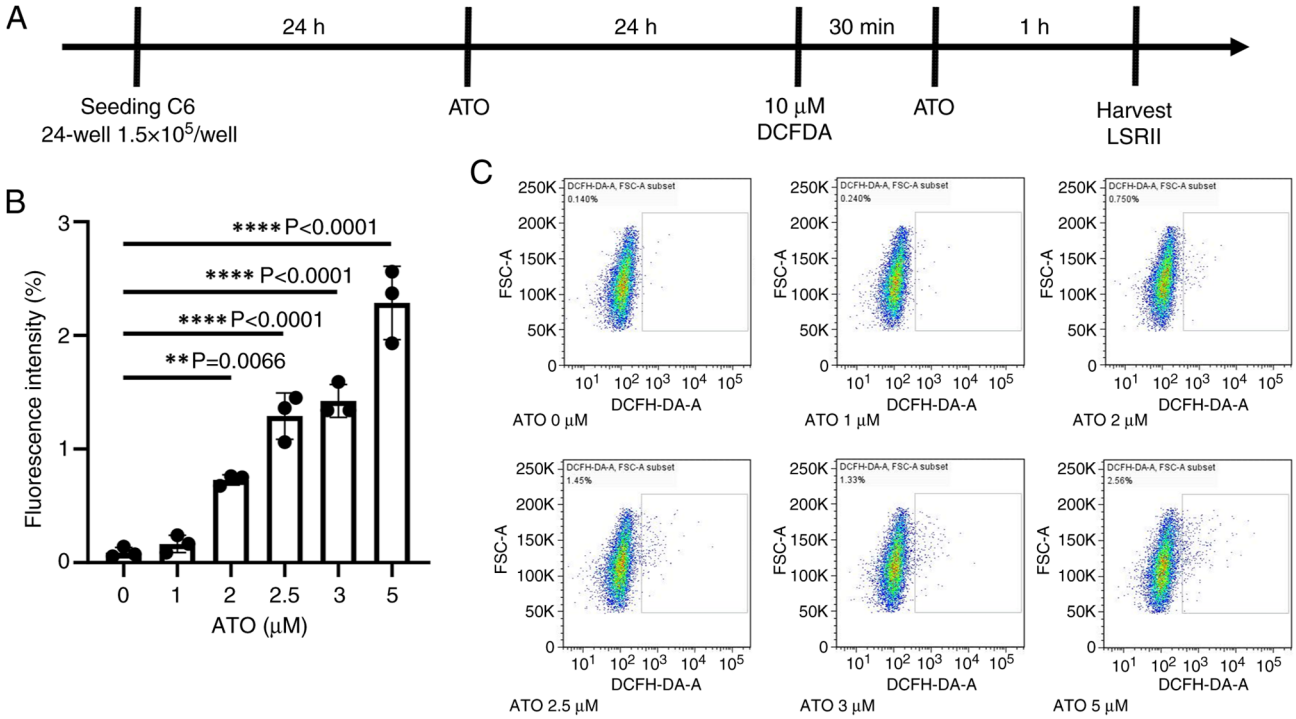

Figure 2. Effect of ATO on the ROS levels of C6 glioma cells. (A) Flow diagram. (B) ROS levels of C6 cells treated with 1, 2, 2.5, 3 and 5 μM, determined by flow cytometry (n=3). (C) Flow cytometry scatter diagrams. **P<0.01, ****P<0.0001. DCFDA, 2',7'-dichlorodihydrofluorescein diacetate; ATO, atorvastatin; ROS, reactive oxygen species.

P<0.0001 for both 5 and 10 μM). Similarly, as shown in Fig. 1D, cell survival progressively decreased with increasing ATO concentrations (1, 2, 2.5, 3 and 5 μM) compared with that in the untreated group. Although treatment with 1 μM ATO indicated no significant difference (P=0.3478), significant reductions were observed at 2 μM and higher concentrations (P=0.005 at 2 μM; P=0.0008 at 2.5 μM; P=0.0006 at 3 μM; and P<0.0001 at 5 μM). There was a significant decrease in cell viability for concentrations ≥2 μM (~90% cell viability) and cell morphology exhibited notable cellular death when ATO concentration exceeded 2 μM (Fig. 1C and E).

A flow diagram of the experimental protocol is shown in Fig. 2A. After 24 h of treatment with ATO, DCFDA was used to detect intracellular ROS levels. There was a significant increase in ROS production in response to ATO at concentrations ≥2 μM (Fig. 2B); compared with in the untreated group, ROS levels were significantly elevated at 2 μM (P=0.0066) and progressively increased at 2.5, 3 and 5 μM (all P<0.0001), which indicated a dose-dependent enhancement in ROS generation (Fig. 2B and C). The C6 cells were pre-treated with ATO for 24 h and then treated with DCFDA for 30 min. When C6 cells were treated with ATO for 1 h, there was an increasing trend in ROS production as the concentration of ATO increased.

Effect of US stimulation on the viability and ROS levels of C6 glioma cells. The C6 glioma cells received US stimulation and cell survival was measured after 1 h. The survival rate of C6 cells treated with different intensities of US (0, 1, 1.5, 2, 2.5 and 3 W/cm^2) was not suppressed when compared with the control group (Fig. 3). Cell morphology did not change after US stimulation despite the use of different intensities

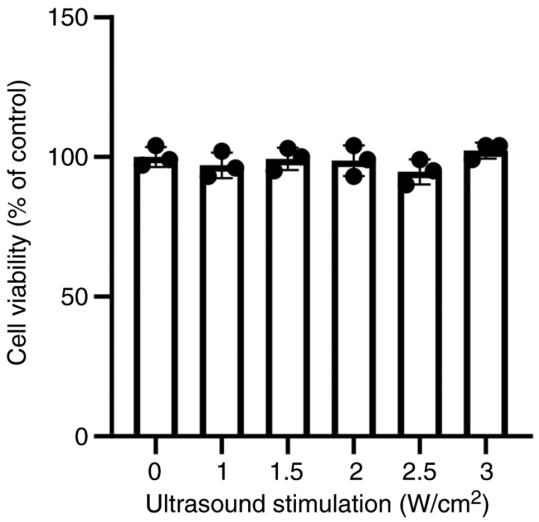

Figure 3. Effect of US stimulation on the viability of C6 cells (n=3). US, ultrasound.

(data not shown). The thermal conditions were also monitored during exposure to different US intensities and no significant temperature elevation was observed (data not shown). A flow diagram of the experimental protocol is shown in Fig. 4A. Cells were pretreated with DCFDA for 30 min and US was delivered for 2 min. Notably, there was no significant change in ROS production when the intensity of US stimulation increased (Fig. 4B and C).

Combined effect of ATO and US on the viability and ROS levels of C6 glioma cells. After pre-treatment with ATO for

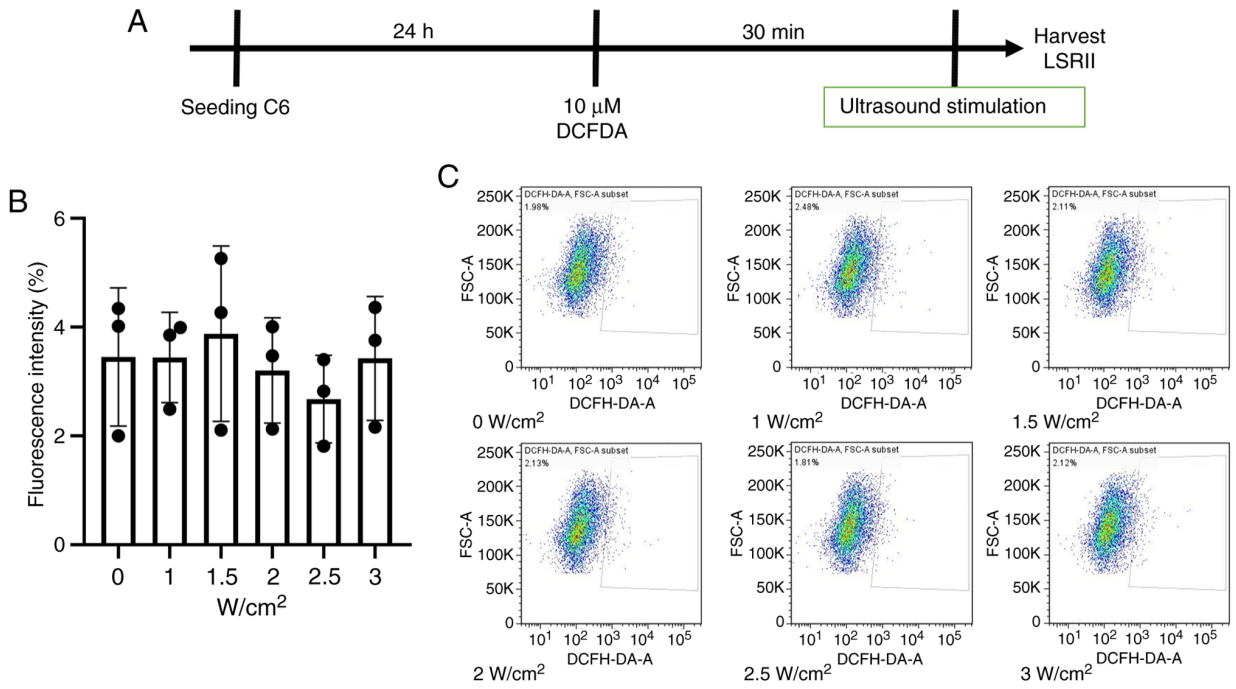

Figure 4. Effect of US stimulation on the ROS levels of C6 glioma cells. (A) Flow diagram. (B) ROS levels of C6 cells treated with 1, 1.5, 2, 2.5 and 3 W/cm^2 US, determined by flow cytometry (n=3). (C) Flow cytometry scatter diagrams. DCFDA, 2',7'-dichlorodihydrofluorescein diacetate; ROS, reactive oxygen species; US, ultrasound.

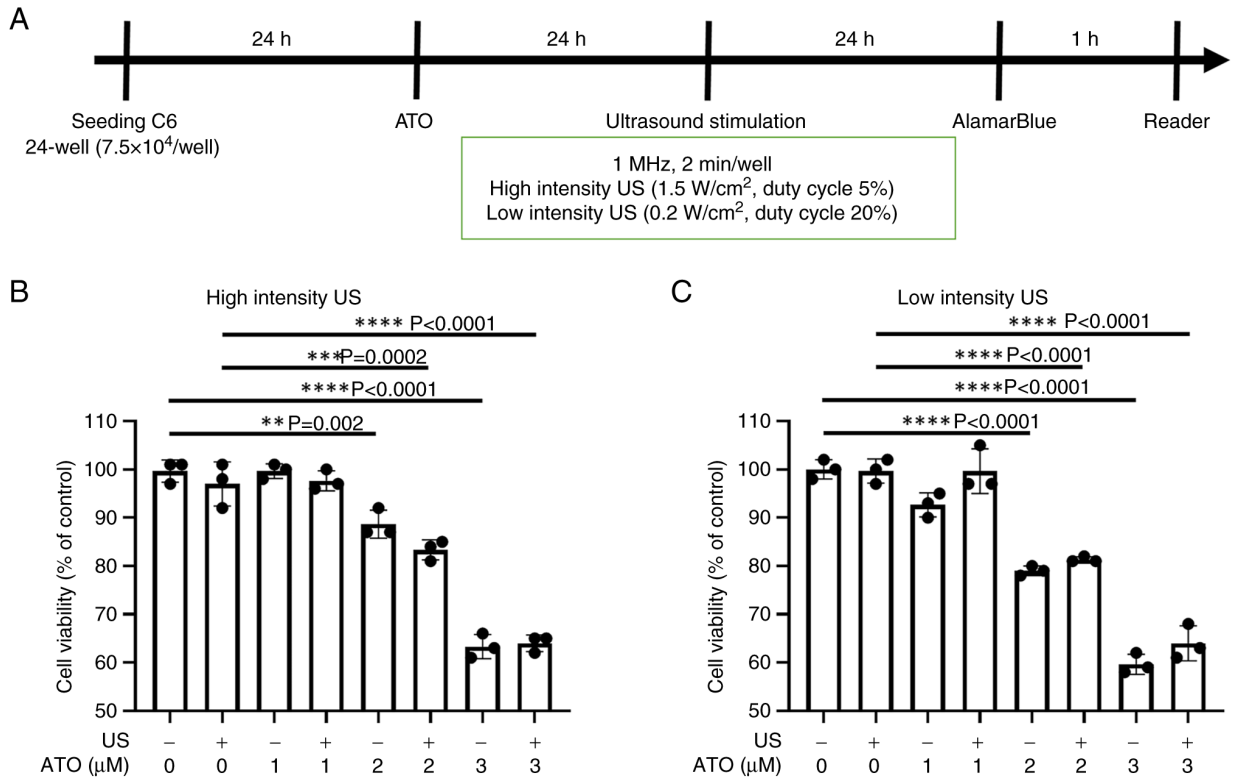

Figure 5. Combined effect of ATO and US on cell viability. (A) Flow diagram. (B) Cell survival in response to ATO combined with high US intensity (1.5 W/cm^2, duty cycle 5%) (n=3). (C) Cell survival in response to ATO combined with low US intensity (0.2 W/cm^2, duty cycle 20%) (n=3). **P<0.01, ***P<0.001, ****P<0.0001. US, ultrasound; ATO, atorvastatin.

24 h, C6 cells were subjected to US stimulation, as per the flow diagram (Fig. 5A). The results of AlamarBlue staining demonstrated that as the concentration of ATO increased, cell viability was suppressed; cell viability was significantly lower in the 2 and 3 μM ATO groups without US compared with that in the untreated control group (P=0.002 and P<0.0001,

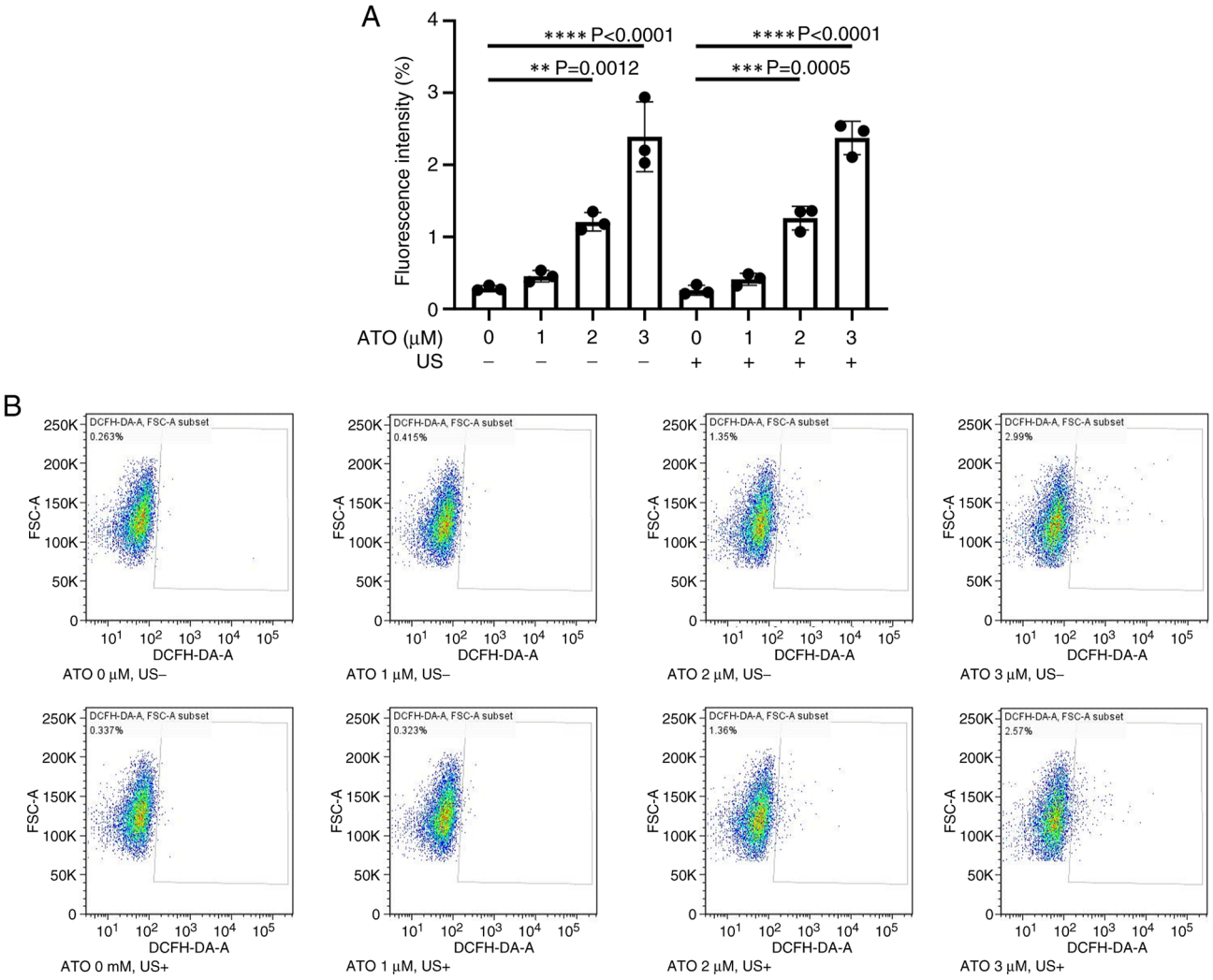

Figure 6. Combined effect of ATO and US on ROS levels. (A) ROS levels (n=3). (B) Flow cytometry scatter diagrams. US intensity was set as 1.5 W/cm^2, duty cycle 5%. **P<0.01, ***P<0.001, ****P<0.0001. ATO, atorvastatin; ROS, reactive oxygen species; US, ultrasound; DCFDA, 2',7'-dichlorodihydrofluorescein diacetate.

respectively; Fig. 5B). A similar pattern was observed when high-intensity US was applied, with a further reductions in cell viability observed in response to 2 and 3 μM ATO compared with that in the control group (P=0.0002 and P<0.0001, respectively). As shown in Fig. 5C, the suppression of cell viability was even more pronounced than in the control group, both without and with low-intensity US exposure, with significantly lower viability in the 2 and 3 μM ATO-treated groups compared with that in the control group (all P<0.0001). However, US stimulation, whether under the condition of high intensity (1.5 W/cm^2, duty cycle 5%) or low intensity (0.2 W/cm^2, duty cycle 20%), did not have a synergistic effect on cell viability when used in combination with ATO. As shown in Fig. 5B and C, no significant differences in cell viability were observed between cells treated with ATO and US compared with those treated with ATO alone across 1, 2 and 3 μM concentrations.

Similar to the experimental process shown in Fig. 2A, for detection of ROS levels, US stimulation was applied before performing flow cytometry. The results indicated that as the concentration of ATO increased, intracellular ROS levels were significantly increased (Fig. 6A and B). ROS levels were significantly higher in the 2 and 3 μM ATO groups compared with those in the untreated control group, both without US (P=0.0012 and P<0.0001, respectively) and with US (P=0.0005 and P<0.0001, respectively). However, stimulation even with high US intensity (1.5 W/cm^2, duty cycle 5%), did not have a synergistic effect on ROS generation when used in combination with ATO.

Effect of ATO and US on mitochondrial ATP production. As shown in Fig. 7, ATP levels were measured after the administration of a control, US, ATO, a combination of US and ATO, and H_2O_2 (positive control). ATP levels were significantly reduced in response to the combination therapy compared with those in the negative control or US groups (P=0.0001; P=0.0003). ATP levels were significantly lower in the ATO-treated group compared with those in the control group (P=0.0008) and were even further reduced in the ATO + US group compared with those in the control group (P=0.0001). When compared with the US group, both the ATO-only group (P=0.0014) and the ATO + US group (P=0.0003) also demonstrated significantly lower ATP levels, which indicated that ATO treatment, with or without US, led to substantial ATP depletion. There was no

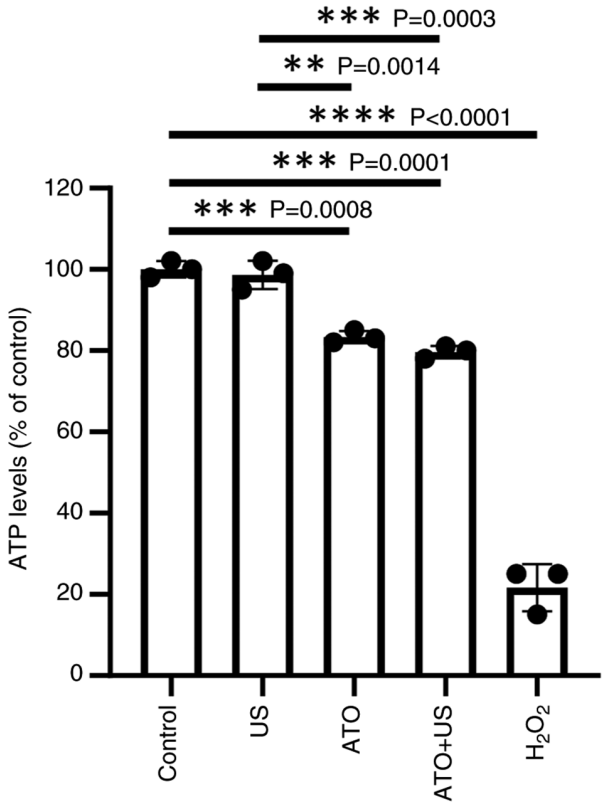

Figure 7. Combined effect of ATO and US on ATP levels (n=3). **P<0.01, ***P<0.001, ****P<0.0001. ATO, atorvastatin; US, ultrasound.

significant difference between the ATO or ATO + US groups, thus indicating that US stimulation did not reduce ATP levels. Furthermore, compared with in the control group, the positive control group exhibited attenuated ATP levels after treatment of H_2O_2.

Effect of ATO and US on tumor cell migration. The migratory ability of C6 cells was assessed using a gap closure assay. Compared with in the control group, cell migration exhibited a decreasing trend in response to both ATO and ATO + US for 18 h, but it was not significant (Fig. 8). Cell migration was not influenced by US stimulation compared with in the negative control group. Furthermore, no significant differences in migration were observed between the ATO + US group and the ATO-only group at 1, 2 and 3 μM concentrations, which indicated that US stimulation did not affect tumor cell migration when combined with ATO.

Effect of ATO and US on the AKT/mTOR pathway. Western blot analysis was performed to detect the expression levels of proteins in the AKT/mTOR pathway, which is associated with apoptosis. Both ATO and combination therapy downregulated the phosphorylation of AKT in C6 cells, which indicated decreased AKT activation (Fig. 9A and B). Notably, the phosphorylation levels were significantly lower in the ATO + US group and the ATO-only group compared with those in the control group (P=0.0094 and P=0.0221, respectively), whereas the US-only group indicated no significant difference compared with the control group (P=0.2458). Furthermore, there was no significant difference between the combination therapy and ATO alone groups (P=0.915), which suggested that US did not further enhance AKT inhibition. The downstream signaling cascade demonstrated a decreasing trend in mTOR activity in the combination therapy group, although the difference was not statistically significant compared with that in the control group (Fig. 9A and C). These results indicated that ATO and combination therapy were associated with the AKT pathway.

Discussion

The present study demonstrated that treatment with ATO suppressed the survival and migration of glioma cells by increasing ROS levels and activating the AKT/mTOR pathway. However, no synergistic effect was observed when ATO was combined with US stimulation. These findings suggested that ATO alone may be considered a potential therapeutic agent for glioma treatment.

Although the present study did not demonstrate an additional benefit of US in glioma cell treatment, US remains a promising therapeutic strategy for glioma treatment due to its complementary mechanisms of action. US has emerged as a potential tool in cancer treatment due to its ability to penetrate tissues and focus energy on specific areas (36). In particular, low-intensity US is employed in sonodynamic therapy (SDT) to activate sensitizing agents and generate cytotoxic effects (7). Previous studies have demonstrated that SDT, when combined with sonosensitizers such as hematoporphyrin monomethyl ether, enhances the therapeutic effect on C6 glioma cells by inducing oxidative stress, disrupting mitochondrial function and activating apoptosis pathways (37,38). Moreover, the US-induced production of ROS serves a key role in damaging tumor cells by targeting cellular membranes and intracellular components, which ultimately lead to cell death (7,39). Another notable advantage of US in cancer therapy is its ability to enhance the permeability of the BBB via transient disruption, which thereby allows for improved delivery of therapeutic agents to the brain (40,41). Additionally, high-intensity focused US offers another therapeutic avenue through thermal ablation (42). This non-invasive approach induces localized heating, which leads to apoptosis in cancer cells. The temperature elevation can exceed 60˚C, which leads to protein denaturation and cellular necrosis (42,43). Nevertheless, the present study did not successfully suppress the tumor survival rate or induce ROS in C6 glioma cells even with the administration of microbubbles; it may be hypothesized that this lack of effect is due to the differences between *in vitro* experimental conditions and *in vivo* or clinical settings.

The present study revealed the effectiveness of low-dose ATO on suppression of tumor survival via ROS generation. ATO, as a member of the statin family, is widely known for its lipid-lowering properties through the inhibition of HMG-CoA reductase. However, beyond its cardiovascular benefits, ATO has demonstrated potential anticancer effects, particularly in glioma treatment via modulation of tumor proliferation, migration, apoptosis and angiogenesis, indicating that it may be a promising candidate for adjuvant cancer therapy (44,45). ATO has been documented to interfere with the mevalonate pathway and inhibit the prenylation

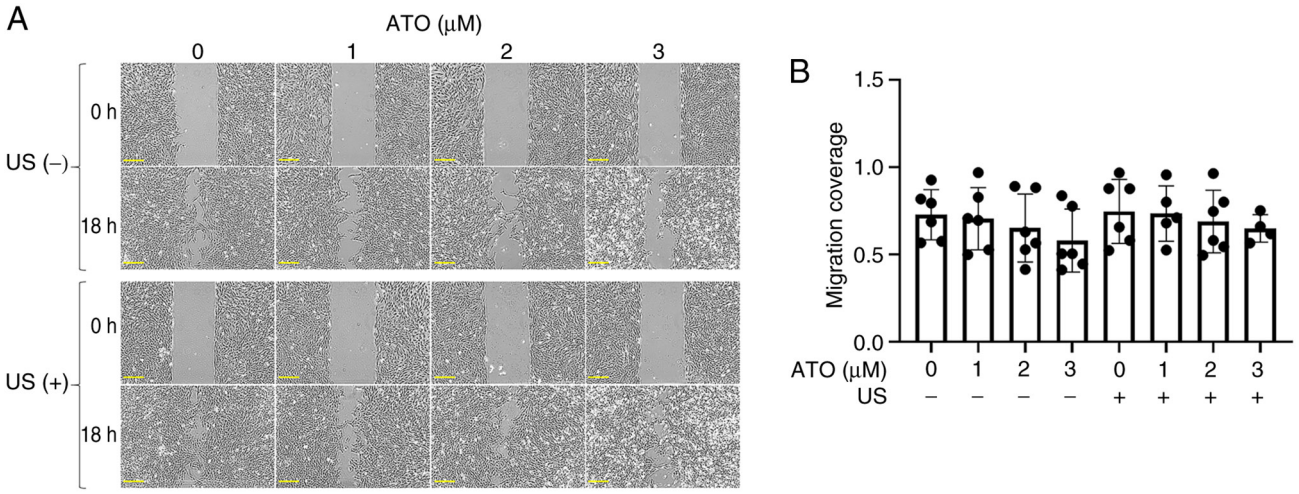

Figure 8. Tumor cell migration experiments. (A) Gap closure assay was used to assess tumor cell migration. Scale bar, 200 μm. (B) Quantification of tumor migration coverage after ATO treatment with or without US (n=6). ATO, atorvastatin; US, ultrasound.

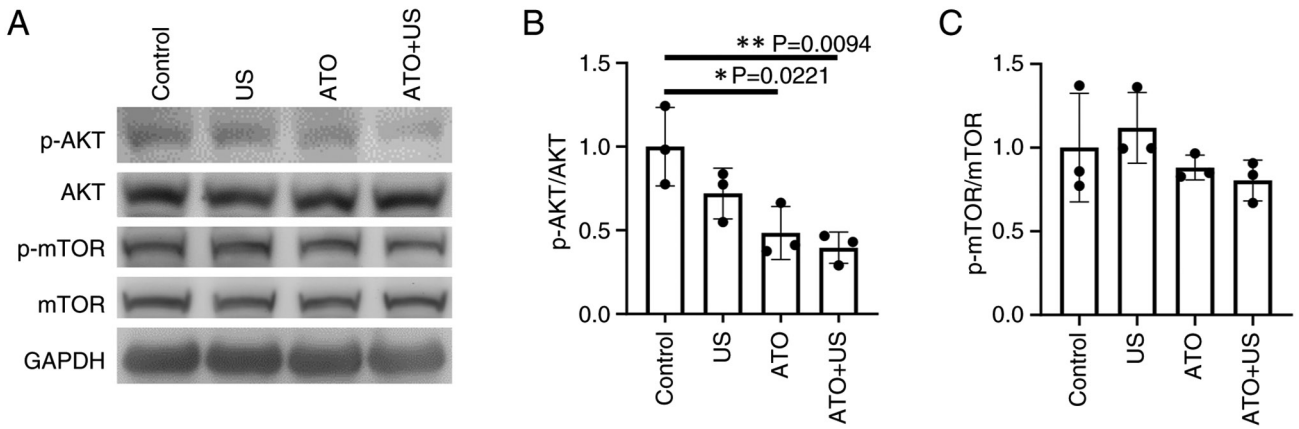

Figure 9. Western blot analysis results. (A) Western blot analysis of proteins associated with the AKT/mTOR pathway. Semi-quantification of (B) p-AKT/AKT (n=3) and (C) p-mTOR/mTOR (n=3). *P<0.05, **P<0.01. ATO, atorvastatin; US, ultrasound; p-, phosphorylated.

of proteins such as Ras, Rac1 and Rho, which serve key roles in tumor growth, migration and apoptosis (28,29,46,47). Moreover, ATO has been shown to inhibit glioma cell migration and invasion, processes that are central to the aggressive nature of GBM (48). The suppression of Ras/Rho signaling pathways, in particular, is key to limiting the invasive behavior of glioma cells, which typically infiltrate surrounding brain tissue, making complete surgical removal difficult (49). ATO also modulates the expression of apoptosis-related proteins (such as caspase-3 and Bcl-2), which promote the activation of pro-apoptotic factors such as Bax and caspase-3, while downregulating anti-apoptotic proteins such as Bcl-2 (50). This dual effect enhances the susceptibility of glioma cells to programmed cell death, which thereby reduces tumor growth and progression (44,50). Additionally, the ability of ATO to reduce cholesterol synthesis in glioma cells is particularly relevant given the role of cholesterol in supporting tumor growth. Glioma cells, similar to several other cancer cells, exhibit a reprogrammed metabolic profile that includes increased cholesterol uptake and synthesis to meet the demands of rapid cell proliferation (16,51). By targeting cholesterol metabolism, ATO not only inhibits the availability of essential lipids for tumor growth but also disrupts the formation of lipid rafts, which are specialized membrane microdomains that are involved in cell signaling and cancer progression (52,53).

Despite the promising results from ATO alone, combining it with US did not demonstrate additional efficacy in terms of cell viability, ROS production or migration. Previous studies have reported on the combination of statins and US-based therapies. In contrast to the present study, which evaluated the effects of ATO (0-5 μM) combined with US at 1 MHz and intensities ≤1 W/cm^2 on C6 glioma cells, previous studies have applied different US parameters and cancer models, which has led to distinct outcomes. Liao *et al* (54) investigated FaDu head and neck cancer cells using pulsed US (1 W/cm^2, six 30-sec bursts) with 12 mg/ml cisplatin-loaded microbubbles in combination with ATO (10-20 μM), and demonstrated notable reductions in cell viability and glutathione levels, indicating a synergistic cytotoxic effect. Xu *et al* (55) used low-frequency US (80 kHz, 0.45 W/cm^2 for 30 sec) in combination with microbubbles and simvastatin (3 μM) in DU145 prostate cancer cells, which resulted in enhanced apoptosis, and downregulation of caveolin-1 and p-AKT. Similarly, Li *et al* (56) employed US at

0.6 W/cm^2 with 20% microbubbles and simvastatin (12 μM) on MCF-7 breast cancer cells, and demonstrated notable apoptosis induction. Compared with these previous studies, the use of relatively high-frequency US (1 MHz) and lower ATO concentrations ($\leq$5 μM) in glioma cells in the present study did not yield a synergistic effect. US typically works by increasing permeability of the BBB for chemotherapy delivery or the promotion of localized heating (41,57), which may not synergize with the biochemical pathways targeted by statins. According to the present results, C6 glioma cells have a threshold response to ATO, which is not further improved by additional physical treatments such as US, thus indicating that the cellular pathways activated by ATO were already maximally engaged at therapeutic doses. In animal models, US has been used to temporarily open the BBB to facilitate drug delivery to the CNS (58). However, the present *in vitro* setting was unable to replicate this condition. Regarding the cell type, GBM cells may have distinct resistance mechanisms and a dense extracellular matrix, which potentially limits the extent of sonoporation and drug penetration compared with other cancer types, such as breast or prostate cancer. Finally, previous studies often observed synergy when US enhanced the intracellular delivery of chemotherapeutics such as cisplatin. By contrast, statins exert their anticancer effects largely through metabolic and redox pathways, such as the mevalonate pathway and glutathione levels, which may not be as sensitive to increased cellular uptake facilitated by microbubble cavitation. Thus, the lack of observable synergy may stem from the mismatch between the mechanisms of ATO action and the mechanical effects induced by US in GBM cells.

ATO, primarily known for its cholesterol-lowering effects, has been highlighted as a potential antitumor agent, particularly against glioma, such as in C6 glioma cells (51). Glioma cells exhibit a unique dependency on cholesterol, which is key for their rapid proliferation, relying on external sources of cholesterol due to their altered metabolic profiles (44,51). By blocking HMG-CoA reductase, ATO reduces the synthesis of cholesterol within glioma cells, which leads to impaired membrane integrity and reduced cellular signaling capabilities, and ultimately hinders tumor growth (45,59). ATO may enhance the efflux of cholesterol from glioma cells by activating liver X receptors to regulate genes (such as ATP-binding cassette sterol transporters ABCG5 and ABCG8) involved in cholesterol transport and metabolism, which promotes the removal of excess cholesterol from cells and potentially leads to reduced tumor aggressiveness (60). By lowering intracellular cholesterol levels, ATO can disrupt lipid raft integrity; this disruption can impair signaling pathways, such as the PI3K/AKT pathway, which promote cell survival and proliferation, which makes glioma cells more susceptible to apoptosis (61,62).

The antitumor effects of ATO are mediated through several key signaling pathways, including the PI3K/AKT, MEK/ERK, mTOR and NF-κB pathways (44,45). The PI3K/AKT signaling pathway is key for cell survival and proliferation. In numerous cancer types, including gliomas, this pathway is often hyperactivated due to mutations in upstream regulators. ATO has been shown to inhibit this pathway by reducing the phosphorylation of AKT or disrupting the interaction between Ras and PI3K (63). This inhibition promotes apoptosis in C6 glioma cells, as lower AKT activity is associated with increased cell death and reduced proliferation (64). In terms of MEK/ERK and Ras/Raf/ERK pathway modulation, ATO has been revealed to inhibit ERK phosphorylation, which is essential for the activation of downstream targets involved in cell proliferation and differentiation (65). By blocking this pathway, ATO reduces the expression of pro-angiogenic factors such as vascular endothelial growth factor and basic fibroblast growth factor, which are often upregulated in tumors (66). Regarding the inhibition of mTOR signaling, ATO has been reported to inhibit mTOR signaling indirectly through its effects on the PI3K/AKT pathway (67). When AKT is inhibited by ATO, downstream mTOR signaling is also suppressed, which leads to reduced protein synthesis and tumor cell proliferation, as well as increased sensitivity to chemotherapy agents for the enhancement of overall therapeutic efficacy (67). Moreover, modulation of the NF-κB pathway by ATO contributes to its ability to induce apoptosis and inhibit tumor growth (68,69). The reduction in NF-κB activity aligns with enhanced expression of pro-apoptotic factors, such as caspase-related cascades, while decreasing levels of anti-apoptotic proteins, such as Bcl-2, in C6 glioma cells specifically (68).

The current study presents several strengths that enhance its scientific value. First, it investigated the combinatory effects of ATO and US stimulation on glioma cells, providing novel insights into their potential interaction. The use of quantitative assays facilitated a mechanistic understanding of the observed cellular responses. The present study also contributed to highlight the antitumor potential of ATO in translational relevance for developing adjunctive glioma therapies. Furthermore, observational clinical studies have highlighted the ongoing controversy surrounding long-term statin use, revealing inconsistent results regarding the association between statins and the incidence or overall survival rates of GBM (18,70-72). While more research is needed to fully understand these relationships, the potential role of ATO as a therapeutic agent in glioma treatment warrants further investigation.

Notably, the present *in vitro* experiments face several limitations that can impact the reliability and applicability of the findings. First, the C6 glioma cell line, derived from rat brain tumors, may not fully replicate the biological behavior, genetic heterogeneity or treatment resistance commonly observed in human GBM. Their growth characteristics, response to treatments, oncogenic signaling pathways and genetic profiles can markedly differ from those in human glioma cells (73). Furthermore, *in vitro* models lack the complex tumor microenvironment present in actual brain tumors, such as dynamic interactions with immune cells, stromal and endothelial cells, vascular structures and the extracellular matrix (73). Second, the concentrations of ATO or US parameters used *in vitro* may not reflect clinically relevant dosages. High concentrations that effectively suppress C6 cell proliferation in culture may not be achievable or safe *in vivo*. Extrapolating the dose-response relationship to *in vivo* conditions is challenging. Finally, common assessments, such as cell viability assays, may not provide a comprehensive view of treatment effects. They fail to account for subtler changes such as alterations in cellular metabolism or apoptosis pathways that might occur without significant changes in cell count. These limitations highlight

the need for careful interpretation of results from current glioma studies and underscore the importance of validating findings through complementary *in vivo* experiments.

In the present study, ATO exhibited notable anticancer effects on glioma cells through various mechanisms, primarily centered around the modulation of key signaling pathways involved in tumor growth and survival. Its ability to enhance the efficacy of therapeutic strategies positions ATO as a potential candidate for adjunctive therapy in the treatment of glioma. Further clinical studies are warranted to fully elucidate the potential benefits of ATO in this context.

In conclusion, the treatment of glioma cells with ATO suppressed their survival by increasing ROS levels and enhancing the tumor cell AKT/mTOR pathway. However, no synergistic effect was observed when combining ATO with US stimulation. These findings indicated that ATO may hold promise as a potential therapeutic agent for glioma treatment.

Acknowledgements

The authors would like to acknowledge the service provided by the Flow Cytometric Analyzing and Sorting Core Facility, National Taiwan University Hospital (Taipei, Taiwan). The present study was presented as a poster at the 18th World Congress of the International Society of Physical and Rehabilitation Medicine, 1-6 June 2024 in Sydney, Australia.

Funding

The present study was supported by the National Science and Technology Council (grant no. NSTC111-2 314-B-002-303-MY2), the National Taiwan University Hospital (grant nos. 114-CTC0013, NTUH 114-X0009, MS469) and the Ministry of Health and Welfare (grant no. MOHW114-TDU-B-211-124001).

Availability of data and materials

The data generated in the present study may be requested from the corresponding author.

Authors' contributions

MTL conceptualized the study, performed data curation, formal analysis and methodology development, wrote the original draft, managed project administration and conducted the investigation. TYC organised the raw datasets and performed formal analysis, methodology and data validation. WHL conceptualized the study, performed methodology and conducted the investigation. CHW performed methodology, and contributed to reviewing and editing the manuscript. THY and WSC performed methodology, contributed to reviewing and editing the manuscript, supplied resources and managed project administration. MTL and TYC confirm the authenticity of all the raw data. All authors read and approved the final manuscript.

Ethics approval and consent to participate

Not applicable.

Patient consent for publication

Not applicable.

Competing interests

The authors declare that they have no competing interests.

References

1. World Health Organization (WHO): ICD-10: International statistical classification of diseases and related health problems/World Health Organization: 10th revision, 2nd edition. WHO, Geneva, 2004.
2. Kanderi T, Munakomi S and Gupta V: Glioblastoma multiforme. In: StatPearls [Internet]. StatPearls Publishing, Treasure Island, FL, 2025.
3. Omuro A and DeAngelis LM: Glioblastoma and other malignant gliomas: A clinical review. JAMA 310: 1842-1850, 2013.
4. Tan AC, Ashley DM, López GY, Malinzak M, Friedman HS and Khasraw M: Management of glioblastoma: State of the art and future directions. CA Cancer J Clin 70: 299-312, 2020.
5. van Tellingen O, Yetkin-Arik B, de Gooijer MC, Wesseling P, Wurdinger T and de Vries HE: Overcoming the blood-brain tumor barrier for effective glioblastoma treatment. Drug Resist Updat 19: 1-12, 2015.
6. Hao D, Song Y, Che Z and Liu Q: Calcium overload and in vitro apoptosis of the C6 glioma cells mediated by sonodynamic therapy (hematoporphyrin monomethyl ether and ultrasound). Cell Biochem Biophys 70: 1445-1452, 2014.
7. Li JH, Chen ZQ, Huang Z, Zhan Q, Ren FB, Liu JY, Yue W and Wang Z: In vitro study of low intensity ultrasound combined with different doses of PDT: Effects on C6 glioma cells. Oncol Lett 5: 702-706, 2013.
8. Liu HL, Huang CY, Chen JY, Wang HYJ, Chen PY and Wei KC: Pharmacodynamic and therapeutic investigation of focused ultrasound-induced blood-brain barrier opening for enhanced temozolomide delivery in glioma treatment. PLoS One 9: e114311, 2014.
9. Wei KC, Chu PC, Wang HY, Huang CY, Chen PY, Tsai HC, Lu YJ, Lee PY, Tseng IC, Feng LY, *et al*: Focused ultrasound-induced blood-brain barrier opening to enhance temozolomide delivery for glioblastoma treatment: A preclinical study. PLoS One 8: e58995, 2013.
10. Lentacker I, De Cock I, Deckers R, De Smedt SC and Moonen CTW: Understanding ultrasound induced sonoporation: Definitions and underlying mechanisms. Adv Drug Deliv Rev 72: 49-64, 2014.
11. Konofagou EE, Tung YS, Choi J, Deffieux T, Baseri B and Vlachos F: Ultrasound-induced blood-brain barrier opening. Curr Pharm Biotechnol 13: 1332-1345, 2012.
12. Honda H, Kondo T, Zhao QL, Feril LB Jr and Kitagawa H: Role of intracellular calcium ions and reactive oxygen species in apoptosis induced by ultrasound. Ultrasound Med Biol 30: 683-692, 2004.
13. Escoffre JM, Campomanes P, Tarek M and Bouakaz A: New insights on the role of ROS in the mechanisms of sonoporation-mediated gene delivery. Ultrason Sonochem 64: 104998, 2020.
14. Liao WH, Wu CH and Chen WS: Pre-treatment with either L-carnitine or piracetam increases ultrasound-mediated gene transfection by reducing sonoporation-associated apoptosis. Ultrasound Med Biol 44: 1257-1265, 2018.
15. Oesterle A, Laufs U and Liao JK: Pleiotropic effects of statins on the cardiovascular system. Circ Res 120: 229-243, 2017.
16. Afshari AR, Mollazadeh H, Henney NC, Jamialahmad T and Sahebkar A: Effects of statins on brain tumors: A review. Semin Cancer Biol 73: 116-133, 2021.
17. Peng P, Wei W, Long C and Li J: Atorvastatin augments temozolomide's efficacy in glioblastoma via prenylation-dependent inhibition of Ras signaling. Biochem Biophys Res Commun 489: 293-298, 2017.
18. Gaist D, Hallas J, Friis S, Hansen S and Sørensen HT: Statin use and survival following glioblastoma multiforme. Cancer Epidemiol 38: 722-727, 2014.

19. Chen BK, Chiu HF and Yang CY: Statins are associated with a reduced risk of brain cancer: A population-based case-control study. Medicine (Baltimore) 95: e3392, 2016.
20. Bouitbir J, Singh F, Charles AL, Schlagowski AI, Bonifacio A, Echaniz-Laguna A, Geny B, Krähenbühl S and Zoll J: Statins trigger mitochondrial reactive oxygen species-induced apoptosis in glycolytic skeletal muscle. Antioxid Redox Signal 24: 84-98, 2016.
21. Bouitbir J, Charles AL, Echaniz-Laguna A, Kindo M, Daussin F, Auwerx J, Piquard F, Geny B and Zoll J: Opposite effects of statins on mitochondria of cardiac and skeletal muscles: A 'mitohormesis' mechanism involving reactive oxygen species and PGC-1. Eur Heart J 33: 1397-1407, 2012.
22. Biselli-Chicote PM, Lotierzo AT, Biselli JM, Paravino EC and Goloni-Bertollo EM: Atorvastatin increases oxidative stress and inhibits cell migration of oral squamous cell carcinoma in vitro. Oral Oncol 90: 109-114, 2019.
23. Parsons DW, Jones S, Zhang X, Lin JC, Leary RJ, Angenendt P, Mankoo P, Carter H, Siu IM, Gallia GL, *et al*: An integrated genomic analysis of human glioblastoma multiforme. Science 321: 1807-1812, 2008.
24. Shi Y, Lim SK, Liang Q, Iyer SV, Wang HY, Wang Z, Xie X, Sun D, Chen YJ, Tabar V, *et al*: Gboxin is an oxidative phosphorylation inhibitor that targets glioblastoma. Nature 567: 341-346, 2019.
25. Liu X, Zhao P, Wang X, Wang L, Zhu Y, Song Y and Gao W: Celastrol mediates autophagy and apoptosis via the ROS/JNK and Akt/mTOR signaling pathways in glioma cells. J Exp Clin Cancer Res 38: 184, 2019.
26. Zhang L, Wang H, Xu J, Zhu J and Ding K: Inhibition of cathepsin S induces autophagy and apoptosis in human glioblastoma cell lines through ROS-mediated PI3K/AKT/mTOR/p70S6K and JNK signaling pathways. Toxicol Lett 228: 248-259, 2014.
27. Yin H, Zhou Y, Wen C, Zhou C, Zhang W, Hu X, Wang L, You C and Shao J: Curcumin sensitizes glioblastoma to temozolomide by simultaneously generating ROS and disrupting AKT/mTOR signaling. Oncol Rep 32: 1610-1616, 2014.
28. Oliveira KA, Dal-Cim T, Lopes FG, Ludka FK, Nedel CB and Tasca CI: Atorvastatin promotes cytotoxicity and reduces migration and proliferation of human A172 glioma cells. Mol Neurobiol 55: 1509-1523, 2018.
29. Bayat N, Ebrahimi-Barough S, Norouzi-Javidan A, Saberi H, Tajerian R, Ardakan MMM, Shirian S, Ai A and Ai J: Apoptotic effect of atorvastatin in glioblastoma spheroids tumor cultured in fibrin gel. Biomed Pharmacother 84: 1959-1966, 2016.
30. Lo CW, Desjouy C, Chen SR, Lee JL, Inserra C, Béra JC and Chen WS: Stabilizing in vitro ultrasound-mediated gene transfection by regulating cavitation. Ultrason Sonochem 21: 833-839, 2014.
31. Brand MD, Orr AL, Perevoshchikova IV and Quinlan CL: The role of mitochondrial function and cellular bioenergetics in ageing and disease. Br J Dermatol 169 (Suppl 2): S1-S8, 2013.
32. Miyoshi N, Watanabe E, Osawa T, Okuhira M, Murata Y, Ohshima H and Nakamura Y: ATP depletion alters the mode of cell death induced by benzyl isothiocyanate. Biochim Biophys Acta 1782: 566-573, 2008.
33. Radstake WE, Gautam K, Van Rompay C, Vermeesen R, Tabury K, Verslegers M, Baatout S and Baselet B: Comparison of in vitro scratch wound assay experimental procedures. Biochem Biophys Rep 33: 101423, 2023.
34. Buachan P, Chularojmontri L and Wattanapitayakul SK: Selected activities of Citrus maxima Merr. fruits on human endothelial cells: Enhancing cell migration and delaying cellular aging. Nutrients 6: 1618-1634, 2014.
35. Liao WH, Hsiao MY, Kung Y, Liu HL, Béra JC, Inserra C and Chen WS: TRPV4 promotes acoustic wave-mediated BBB opening via Ca^{2+}/PKC-δ pathway. J Adv Res 26: 15-28, 2020.
36. Wood AKW and Sehgal CM: A review of low-intensity ultrasound for cancer therapy. Ultrasound Med Biol 41: 905-928, 2015.
37. Chen H, Zhou X, Gao Y, Zheng B, Tang F and Huang J: Recent progress in development of new sonosensitizers for sonodynamic cancer therapy. Drug Discov Today 19: 502-509, 2014.
38. Shibaguchi H, Tsuru H, Kuroki M and Kuroki M: Sonodynamic cancer therapy: A non-invasive and repeatable approach using low-intensity ultrasound with a sonosensitizer. Anticancer Res 31: 2425-2429, 2011.
39. Liang L, Xie S, Jiang L, Jin H, Li S and Liu J: The combined effects of hematoporphyrin monomethyl ether-SDT and doxorubicin on the proliferation of QBC939 cell lines. Ultrasound Med Biol 39: 146-160, 2013.
40. Burgess A and Hynynen K: Drug delivery across the blood-brain barrier using focused ultrasound. Expert Opin Drug Deliv 11: 711-721, 2014.
41. Liu HL, Fan CH, Ting CY and Yeh CK: Combining microbubbles and ultrasound for drug delivery to brain tumors: Current progress and overview. Theranostics 4: 432-444, 2014.
42. Hsiao YH, Kuo SJ, Tsai HD, Chou MC and Yeh GP: Clinical application of high-intensity focused ultrasound in cancer therapy. J Cancer 7: 225-231, 2016.
43. Maloney E and Hwang JH: Emerging HIFU applications in cancer therapy. Int J Hyperthermia 31: 302-309, 2015.
44. Alrosan AZ, Heilat GB, Al Subeh ZY, Alrosan K, Alrousan AF, Abu-Safieh AK and Alabdallat NS: The effects of statin therapy on brain tumors, particularly glioma: A review. Anticancer Drugs 34: 985-994, 2023.
45. Rendon LF, Tewarie IA, Cote DJ, Gabriel A, Smith TR, Broekman MLD and Mekary RA: Statins and gliomas: A systematic review of the preclinical studies and meta-analysis of the clinical literature. Drugs 82: 293-310, 2022.
46. Bayat N, Ebrahimi-Barough S, Norouzi-Javidan A, Saberi H, Ardakan MMM, Ai A, Soleimannejad M and Ai J: Anti-inflammatory effects of atorvastatin in human glioblastoma spheroids cultured in a three-dimensional model: Possible relevance to glioblastoma treatment. Mol Neurobiol 55: 2102-2110, 2018.
47. Yongjun Y, Shuyun H, Lei C, Xiangrong C, Zhilin Y and Yiquan K: Atorvastatin suppresses glioma invasion and migration by reducing microglial MT1-MMP expression. J Neuroimmunol 260: 1-8, 2013.
48. Lübtow MM, Oerter S, Quader S, Jeanclos E, Cubukova A, Krafft M, Haider MS, Schulte C, Meier L, Rist M, *et al*: In vitro blood-brain barrier permeability and cytotoxicity of an atorvastatin-loaded nanoformulation against glioblastoma in 2D and 3D models. Mol Pharm 17: 1835-1847, 2020.
49. Afshordel S, Kern B, Clasohm J, König H, Priester M, Weissenberger J, Kögel D and Eckert GP: Lovastatin and perillyl alcohol inhibit glioma cell invasion, migration, and proliferation-impact of Ras-/Rho-prenylation. Pharmacol Res 91: 69-77, 2015.
50. Zhang L, Chen T, Dou Y, Zhang S, Liu H, Khishignyam T, Li X, Zuo D, Zhang Z, Jin M, *et al*: Atorvastatin exerts antileukemia activity via inhibiting mevalonate-YAP axis in K562 and HL60 cells. Front Oncol 9: 1032, 2019.
51. Guo X, Zhou S, Yang Z, Li ZA, Hu W, Dai L, Liang W and Wang X: Cholesterol metabolism and its implication in glioblastoma therapy. J Cancer 13: 1745-1757, 2022.
52. Murai T, Maruyama Y, Mio K, Nishiyama H, Suga M and Sato C: Low cholesterol triggers membrane microdomain-dependent CD44 shedding and suppresses tumor cell migration. J Biol Chem 286: 1999-2007, 2011.
53. Bomben VC, Turner KL, Barclay TTC and Sontheimer H: Transient receptor potential canonical channels are essential for chemotactic migration of human malignant gliomas. J Cell Physiol 226: 1879-1888, 2011.
54. Liao AH, Lin WT, Chen HK, Shih CP, Wang CH and Chu YH: Synergistic effects of combined treatment with ultrasound-mediated cisplatin-loaded microbubbles and atorvastatin on head and neck cancer. Head Neck 43: 15-26, 2021.
55. Xu WP, Shen E, Bai WK, Wang Y and Hu B: Enhanced antitumor effects of low-frequency ultrasound and microbubbles in combination with simvastatin by downregulating caveolin-1 in prostatic DU145 cells. Oncol Lett 7: 2142-2148, 2014.
56. Li H, Chen C and Wang D: Low-frequency ultrasound and microbubbles combined with simvastatin promote the apoptosis of MCF-7 cells by affecting the LATS1/YAP/RHAMM pathway. Mol Med Rep 18: 2724-2732, 2018.
57. Kujawska T, Secomski W, Bilmin K, Nowicki A and Grieb P: Impact of thermal effects induced by ultrasound on viability of rat C6 glioma cells. Ultrasonics 54: 1366-1372, 2014.
58. Burgess A, Shah K, Hough O and Hynynen K: Focused ultrasound-mediated drug delivery through the blood-brain barrier. Expert Rev Neurother 15: 477-491, 2015.
59. Maxfield FR and van Meer G: Cholesterol, the central lipid of mammalian cells. Curr Opin Cell Biol 22: 422-429, 2010.
60. Wang B and Tontonoz P: Liver X receptors in lipid signalling and membrane homeostasis. Nat Rev Endocrinol 14: 452-463, 2018.
61. Ponce J, de la Ossa NP, Hurtado O, Millan M, Arenillas JF, Dávalos A and Gasull T: Simvastatin reduces the association of NMDA receptors to lipid rafts: A cholesterol-mediated effect in neuroprotection. Stroke 39: 1269-1275, 2008.

62. Wu H, Jiang H, Lu D, Xiong Y, Qu C, Zhou D, Mahmood A and Chopp M: Effect of simvastatin on glioma cell proliferation, migration, and apoptosis. Neurosurgery 65: 1087-1097, 2009.
63. Liu M, Tang R and Jiang Y: Study on the function and mechanism of atorvastatin in regulating leukemic cell apoptosis by the PI3K/Akt pathway. Int J Clin Exp Med 8: 3371-3380, 2015.
64. Yang D, Han Y, Zhang J, Chopp M and Seyfried DM: Statins enhance expression of growth factors and activate the PI3K/Akt-mediated signaling pathway after experimental intracerebral hemorrhage. World J Neurosci 2: 74-80, 2012.
65. Lo HW: Targeting Ras-RAF-ERK and its interactive pathways as a novel therapy for malignant gliomas. Curr Cancer Drug Targets 10: 840-848, 2010.
66. Adamičková A, Chomaničová N, Gažová A, Maďarič J, Červenák Z, Valášková S, Adamička M and Kyselovic J: Effect of atorvastatin on angiogenesis-related genes VEGF-A, HGF and IGF-1 and the modulation of PI3K/AKT/mTOR transcripts in bone-marrow-derived mesenchymal stem cells. Curr Issues Mol Biol 45: 2326-2337, 2023.
67. Kumar N and Mandal CC: Cholesterol-lowering drugs on Akt signaling for prevention of tumorigenesis. Front Genet 12: 724149, 2021.
68. Tu J, Fang Y, Han D, Tan X, Jiang H, Gong X, Wang X, Hong W and Wei W: Activation of nuclear factor-κB in the angiogenesis of glioma: Insights into the associated molecular mechanisms and targeted therapies. Cell Prolif 54: e12929, 2021.
69. Ortego M, Bustos C, Hernández-Presa MA, Tuñón J, Díaz C, Hernández G and Egido J: Atorvastatin reduces NF-kappaB activation and chemokine expression in vascular smooth muscle cells and mononuclear cells. Atherosclerosis 147: 253-261, 1999.
70. Cote DJ, Rosner BA, Smith-Warner SA, Egan KM and Stampfer MJ: Statin use, hyperlipidemia, and risk of glioma. Eur J Epidemiol 34: 997-1011, 2019.
71. Happold C, Gorlia T, Nabors LB, Erridge SC, Reardon DA, Hicking C, Picard M, Stupp R and Weller M; EORTC Brain Tumor Group and on behalf of the CENTRIC and CORE Clinical Trial Groups: Do statins, ACE inhibitors or sartans improve outcome in primary glioblastoma? J Neurooncol 138: 163-171, 2018.
72. Seliger C, Schaertl J, Gerken M, Luber C, Proescholdt M, Riemenschneider MJ, Leitzmann MF, Hau P and Klinkhammer-Schalke M: Use of statins or NSAIDs and survival of patients with high-grade glioma. PLoS One 13: e0207858, 2018.
73. Barth RF and Kaur B: Rat brain tumor models in experimental neuro-oncology: The C6, 9L, T9, RG2, F98, BT4C, RT-2 and CNS-1 gliomas. J Neurooncol 94: 299-312, 2009.